atmosphere of CO. The orange solution, which immediately became yellow, was stirred for 2 h. Hexane (ca. 15 mL) was then added until a lemon yellow solid precipitated. This was filtered off, washed with hexane (2 × 5 mL), and dried. Yield: 0.040 g (0.041 mmol), 81%. Anal. Calcd for $C_{42}H_{39}As_3ClORu \cdot {}^1/_5CH_2Cl_2$: C, 52.06; H, 4.09; Cl, 8.74. Found: C, 51.73; H, 4.08; Cl, 9.11. The presence of CH_2Cl_2 in the indicated ratio was confirmed by ^1H NMR in $CDCl_3$.

[Ru(CF$_3$SO$_3$)(CO)$_2$(triphos)](CF$_3$SO$_3$) (9). A yellow CH_2Cl_2 solution (5 mL) of $[Ru(H_2O)(DMSO)_2(triphos)](CF_3SO_3)_2$ (0.050 g, 0.042 mmol) was freeze–thaw–degassed three times and then stirred under an atmosphere of CO. The solution, which became colorless within 5 min, was stirred for an additional 10 min to ensure complete reaction. Addition of diethyl ether (ca. 10 mL) with vigorous stirring gave a colorless solid, which was filtered, washed with diethyl ether, and dried. Yield: 0.041 g, (0.038 mmol), 90%. Anal. Calcd for $C_{45}H_{39}F_6O_8P_3RuS_2$: C, 50.04; H, 3.65. Found: C, 49.70; H, 3.57.

[Ru(CF$_3$SO$_3$)(CO)$_2$(triars)](CF$_3$SO$_3$) (10). Complex **10** was prepared analogously to **9**, i.e., by keeping $[Ru(DMSO)_3(triars)](CF_3SO_3)_2$ (0.026 g, 0.020 mmol) under 1 atm of CO, in CH_2Cl_2 for 3 h. Yield: 0.021 g (0.017 mmol), 87%. Anal. Calcd for $C_{45}H_{39}As_3F_6O_8RuS_2$: C, 44.60; H, 3.25. Found: C, 44.29; H, 3.33.

[RuCl(CO)$_2$(triphos)](CF$_3$SO$_3$) (11). Addition of 1 equiv of $NEt_4Cl \cdot 2H_2O$ to a colorless CH_2Cl_2 solution of $[Ru(CF_3SO_3)(CO)_2(triphos)](CF_3SO_3)$ gave a pale yellow solution, from which the solvent was removed in vacuo after 30 min of stirring. A white powder was isolated from an acetone solution of the residual as described by Siegl et al.[9] IR (CsI), cm^{-1}: ν(CO) 2079 s. $^{31}P\{^1H\}$ NMR (CH_2Cl_2): δ 26.24 t (J = 32 Hz, 1 P), −2.28 d (J = 32 Hz, 2 P).

[RuCl$_2$(CO)(triphos)] (12). Addition of 2 equiv of $NEt_4Cl \cdot 2H_2O$ to a colorless CH_2Cl_2 solution of $[Ru(CF_3SO_3)(CO)_2(triphos)](CF_3SO_3)$ gave a yellow precipitate, which was isolated from the cooled solution as described by Siegl et al.[9] IR (CsI), cm^{-1}: ν(CO) 2008 s; ν(Cl) 291 w, 275 w, sh. $^{31}P\{^1H\}$ NMR (CH_2Cl_2): δ +27.80 d (J = 41 Hz, 2 P), −7.83 t (J = 41 Hz, 1 P).

Collection and Reduction of X-ray Intensity Data. The X-ray analysis was undertaken on yellow crystals grown by slow evaporation of a solution of the complex in CH_2Cl_2–MeOH. They are orthorhombic and belong to the space group *Pccn*, as apparent from systematic absences (*h0l* for $l = 2n$, *0kl* for $l = 2n$, and *hk0* for $h + k = 2n$). A prismatic crystal of 0.12 × 0.14 × 0.37 mm approximate dimensions was selected for the collection of the intensities on a Nicolet R3 computer-controlled diffractometer using Mo Kα (λ = 0.71069 Å) graphite-monochromatized radiation. Cell dimensions, determined by least-squares refinement of the setting angles of 15 carefully centered reflections, are a = 19.991 (8) Å, b = 18.388 (7) Å, c = 25.510 (10) Å, and V = 9377 Å^3. The calculated density is 1.330 g cm^{-3} for Z = 4. The data collection was made by an ω-scan mode with scan range 0.8° and variable scan speed according to the intensities. The background counts were measured for half of the scan time with an offset of 1°.

Three standard reflections were measured every 100 reflections. Their intensities remained constant during the whole data collection. The intensities were processed as already described[44] by using an ignorance factor of p = 0.009 and correcting for shape anisotropy (μ(Mo Kα) = 5.5 cm^{-1}). From a total of 12 720 reflections collected ($3° \geq 2\theta \geq 50°$), a unique set of 3200, having $I \geq 3\sigma(I)$, were considered as observed and used in subsequent calculations. The crystallographic and data collection parameters are summarized in Table IV.

Solution and Refinement of the Structure. The structure was solved by the usual combination of Patterson and Fourier methods. The isotropic refinement converged at R = 0.081. Afterward, the hydrogen contributions were taken into account, and all the non-hydrogen atoms were allowed to vibrate anisotropically. The refinement converged at R = 0.057 and R_w = 0.069. A final electron density map did not reveal any residual peaks. The refinement was carried out with a full matrix, and the function minimized was $\sum w(|F_o| - |F_c|)^2$ with $w = 4F_o^2/\sigma^2(F_o)^2$. Scattering factors and anomalous dispersion terms were taken from ref 45. The calculations were carried out on the Data General Eclipse MV8000II computer using local programs. Final positional parameters of the non-hydrogen atoms are listed in Table V. Anisotropic thermal parameters and a listing of observed and calculated structure factors are available as supplementary material.

Acknowledgment. We thank Professor A. Ludi for communicating his results before publication, F. Bangerter for recording the ^{19}F NMR spectra, and the "Forschungkomission der ETH" (L.F.R.) and the "Schweizerischer Nationalfonds" (C.S.) for financial support.

Registry No. **1**, 103500-17-0; **2**, 112220-32-3; **3**, 112220-33-4; **4**, 103500-16-9; **5**, 109124-78-9; **6a**, 112220-35-6; **6b**, 112220-37-8; **7a**, 112220-39-0; **7b**, 112220-41-4; **8**, 112220-42-5; **9**, 112220-44-7; **10**, 112220-46-9; **11**, 112220-47-0; **14**, 37843-35-9; $[Ru_2(\mu\text{-}Cl)_3(triphos)_2][BPh_4]$, 112220-49-2; $[RuCl_2(DMSO)_4]$, 59091-96-2.

Supplementary Material Available: Figure S1, showing a perspective view of all the heavy atoms of the cationic complex, and Table S1, containing anisotropic thermal parameters (3 pages); Table S2, listing observed and calculated structure factors (20 pages). Ordering information is given on any current masthead page.

(44) Bachechi, F.; Zambonelli, L.; Marcotrigiano, G. *J. Cryst. Mol. Struct.* **1977**, *7*, 11.
(45) *International Tables for X-Ray Crystallography*; Kynoch: Birmingham, England, 1974; Vol. IV.

Contribution from Gorlaeus Laboratories, State University Leiden, P.O. Box 9502, 2300 RA Leiden, The Netherlands

Crystal Structure Determination of Dipotassium Dihydroxotrioxoruthenate(VI): Configuration of the Ruthenate Ion and Its Electronic Properties

M. O. Elout, W. G. Haije, and W. J. A. Maaskant*

Received September 17, 1987

A crystal structure determination has been performed on the compound formerly called dipotassium ruthenate hydrate. This determination revealed a five-coordinate ruthenium, with three equatorial oxygens and two apical hydroxyl ions in a trigonal-bipyramidal arrangement, with symmetry approximately D_{3h}. The dimensions of the orthorhombic unit cell are a = 8.012 (2) Å, b = 10.588 (8) Å, and c = 6.687 (3) Å, in space group $P2_12_12_1$ and with Z = 4. It is shown that this structure is related to that of $BaRuO_3(OH)_2$. Molecular orbital energy levels have been calculated in the arrangement found according to the modified Wolfsberg–Helmholz method. The results of this calculation have been used to interpret the ligand field spectrum of the $RuO_3(OH)_2^{2-}$ ion and are in agreement with the magnetic susceptibility data from which followed that g = 1.93 and S = 1. It is shown that the previous lack of resemblance between calculated and measured spectra of $RuO_3(OH)_2^{2-}$ is mainly due to the erroneous assumption of tetrahedral coordination of the ruthenium ion.

Introduction

Until about 10 years ago, ruthenate was generally believed to occur only as tetraoxo anions, as reflected in the description of its chemistry[1] in the interpretation of ligand field spectra[2-6] and vibrational spectra.[7,8] However, in 1976 it was shown[9] that in $BaRuO_4 \cdot H_2O$ the Ru(VI) ion is coordinated by five oxygens, in

(1) Seddon, E. A.; Seddon, K. R. *The Chemistry of Ruthenium*; Elsevier: Amsterdam, 1984; pp 71–75. Krauss, F. *Z. Anorg. Allg. Chem.* **1924**, *132*, 301.
(2) Carrington, A.; Jørgensen, C. K. *Mol. Phys.* **1961**, *4*, 395.
(3) Viste, A.; Gray, H. B. *Inorg. Chem.* **1964**, *3*, 1113. Connick, R. E.; Hurley, C. R. *J. Am. Chem. Soc.* **1952**, *74*, 5012.
(4) Gray, H. B. *Coord. Chem. Rev.* **1966**, *1*, 2.
(5) Zeigler, T.; Rauk, A.; Baerends, E. J. *Chem. Phys.* **1976**, *16*, 209.
(6) Rauk, A.; Zeigler, T.; Ellis, D. E. *Theor. Chim. Acta* **1974**, *34*, 49.

0020-1669/88/1327-0610$01.50/0

Table I. Structure Determination Data of $K_2RuO_3(OH)_2$

empirical formula	$K_2RuO_5H_2$
mol wt	261.21 g/mol
measuring temp	293 K
cryst class	orthorhombic
space group	$P2_12_12_1$
systematic absences	$h00$, $h = 2n + 1$; $0k0$, $k = 2n + 1$; $00l$, $l = 2n + 1$
lattice const	a = 8.012 (2) Å b = 10.588 (8) Å c = 6.687 (3) Å
vol	567.3 (5) Å^3
cryst size	0.58 mm × 0.56 mm × 0.17 mm
calcd density	3.069 g/cm^3
Z	4
μ	41.16 cm^{-1}
diffractometer syst	Enraf-Nonius CAD4
radiation	Mo Kα with graphite monochromator (λ = 0.71069 Å)
data collcn method	bisect (zigzag)
scan range	1.035° (min), 2.732° (max)
check reflns	−1,−6,0; 4,−3,0; 2,−2,3
abs cor	empirical
transmission	0.2913 (min), 0.4254 (max)
$F(000)$	492
total no. of reflns	4792
2θ(max)	60°
no. of unique reflns	4789; 3372 obsd, 1417 not signif
soln technique	Patterson function, Fourier synth
R	0.0315
R_w	0.0393
Δ/σ (mean)	0.0005
Δ/σ (max)	0.053
total no. of params refined	72
thermal params	anisotropic
H atoms	not calcd

a trigonal bipyramid, and that the correct structural formula is $BaRuO_3(OH)_2$. To gain more insight in related ruthenium compounds, $K_2RuO_3(OH)_2$, formerly known as $K_2RuO_4{\cdot}H_2O$, has been synthesized and some of its structural and electronic properties have been examined.

As it turned out, in this compound the ruthenate anion also appeared to consist of five-coordinated Ru(VI).

To examine its electronic structure qualitatively, an MO calculation was performed, as described by Viste and Gray.[3]

To confirm the MO results, magnetic susceptibility data have been collected in the temperature region from 86 to 304 K to determine the spin quantum number of the ruthenium ion. Furthermore, the visible–UV spectrum of the ruthenate ion[10] has been interpreted.

Experimental Section

Potassium ruthenate has been synthesized according to the method of Krauss[1] from molten KOH in a nickel crucible, to which equimolar amounts of Ru and KNO_3 had been added. After it was cooled, the red mixture was dissolved in water, and by slow evaporation over P_2O_5, deep red air-sensitive crystals were obtained.

A single crystal of dimensions 0.58 mm × 0.56 mm × 0.27 mm has been mounted on an Enraf-Nonius CAD4 diffractometer. The unit cell, determined with 24 reflections, appeared to be orthorhombic, space group $P2_12_12_1$, with lattice constants a = 8.012 (2) Å, b = 10.588 (8) Å, c = 6.687 (3) Å, V = 567.3 (5) Å^3, and ρ = 3.06 g/cm^3 (Z = 4).

Data collection conditions and parameters are given in Table I. Absorption correction according to De Graaff,[11] a correction for the decay of the scattering power, and Lp effects were applied. Scattering factors were taken from ref 12 with correction for the real and imaginary part of the anomalous dispersion. The function minimized during the least-squares refinement was $\sum w(|F_o| - |F_c|)^2$, with $w = 1/\sigma(F)^2$, $\sigma(F)$ being the esd calculated from counting statistics and estimated errors in the aforementioned corrections. For all the calculations computer programs written or modified by Rutten-Keulemans and De Graaff were used on the Leiden University IBM 3081 computer.

The position of the ruthenium ion was determined from the most intense Harker peaks in the Patterson function. First, the two potassium atoms and then the five oxygen atoms were determined in subsequent Fourier maps. These results led to an R_w value of 0.046 in the least-squares refinement. Inspection of F_o and F_c showed that correction for secondary extinction was necessary. The correct enantiomorph was selected by using the anomalous dispersion of the potassium and ruthenium atoms (R_w = 0.040 and 0.039 respectively). In the difference Fourier two peaks remained, corresponding to an electron density of 1.1 e/Å^3 lying at a distance of about 0.8 Å from the Ru ion. Most likely these peaks are due to the nonspherical electron distribution of the ruthenium atom. The hydrogen positions could not be obtained unambiguously from the remaining peaks.

Two Ru–O distances were found: three of approximately 1.8 Å for the equatorial oxygen atoms and two of approximately 2.0 Å for the apical oxygen atoms. As there are also three oxygen ions and two hydroxyl ions, it seems very likely that the hydrogens are bonded to the apical oxygen atoms.

Magnetic susceptibility data were collected on automated Faraday equipment, consisting of a compensating Mettler ME21 microbalance, a furnace with a chromel–alumel thermocouple, and an Oxford Instruments magnet. The apparatus was calibrated with $HgCo(SCN)_4$.[13] The magnetic susceptibility of a sample of 261.1 mg of powdered $K_2RuO_3(OH)_2$ has been measured in the temperature range from 86 to 304 K.

Table II. Coordinates and B(iso) Values (10^{-4} Å^2) of $K_2RuO_3(OH)_2$[a]

atom	x/a	y/b	z/c	B(iso)[b]
K1	3990 (1)	9569 (1)	1280 (1)	172 (1)
K2	2561 (1)	6906 (1)	4596 (1)	187 (1)
Ru	−617 (0)	8819 (0)	915 (0)	107 (0)
O1	4589 (3)	9492 (2)	5191 (3)	164 (4)
O2	745 (3)	8724 (2)	2980 (3)	196 (4)
O3	3448 (3)	7898 (2)	8277 (4)	170 (4)
O4	4911 (3)	6760 (2)	1470 (3)	187 (4)
O5	2419 (3)	5532 (2)	8653 (4)	205 (5)

[a] Estimated standard deviations in the least significant digits are given in parentheses. [b] $B(\text{iso}) = (8\pi^2/3)(U_{11} + U_{22} + U_{33})$.

Table III. Interatomic Distances (Å) and Bond Angles (deg) in $K_2RuO_3(OH)_2$

	Bond Distances		
Ru–O2	1.763 (2)	O1–O2	2.670 (3)
Ru–O4	1.760 (2)	O1–O4	2.675 (4)
Ru–O5	1.741 (2)	O1–O5	2.749 (3)
Ru–O1	2.028 (2)	O1–O3	4.066 (4)
Ru–O3	2.040 (2)		
	Bond Angles		
O1–Ru–O3	177.3 (1)	O2–Ru–O4	122.8 (1)
O1–Ru–O2	89.3 (1)	O2–Ru–O5	116.9 (1)
O1–Ru–O4	89.6 (1)	O4–Ru–O5	120.3 (1)
O1–Ru–O5	93.4 (1)		
	Interionic Distances		
O1–O3	2.819 (3)	K1–K2	3.755 (2)
K1–Ru	3.771 (2)		

Results

The crystal structure determination revealed a five-coordinate ruthenium atom, with three oxygen atoms at a distance of 1.76 Å and two oxygen atoms at 2.03 Å, to which the hydrogen atoms are most likely bonded. The trigonal bipyramid is slightly distorted, as the O–Ru–O angle of the apical oxygen ions is not 180° but 177.3 (1)° and the three O–Ru–O angles of the equatorial oxygen atoms are not all 120° but 120.3 (1), 116.9 (1), and 122.8 (1)°. It should be noted, however, that the equatorial oxygen atoms and the ruthenium atom are coplanar.

(7) Griffith, W. P. *J. Chem. Soc. A* **1966**, 1467.
(8) Gonzalez-Vilchez, F.; Griffith, W. P. *J. Chem. Soc., Dalton Trans.* **1972**, 1416.
(9) Nowogrocki, G.; Abraham, F.; Trehoux, J.; Thomas, D. *Acta Crystallogr., Sect. B: Struct. Crystallogr. Cryst. Chem.* **1976**, *B32*, 2413.
(10) Carrington, A.; Symons, M. C. R. *Chem. Rev.* **1963**, *63*, 443.
(11) De Graaff, R. A. G. *Acta Crystallogr., Sect. A: Cryst. Phys., Diffr., Theor. Gen. Crystallogr.* **1973**, *A29*, 298.
(12) *International Tables for X-ray Crystallography*; Kynoch: Birmingham, England, 1974; Vol. IV; (present distributor D. Reidel, Dordrecht, The Netherlands).
(13) Brown, D. B.; Crawford, V. H.; Hall, J. W.; Hatfield, W. E. *J. Phys. Chem.* **1977**, *81*, 1303.

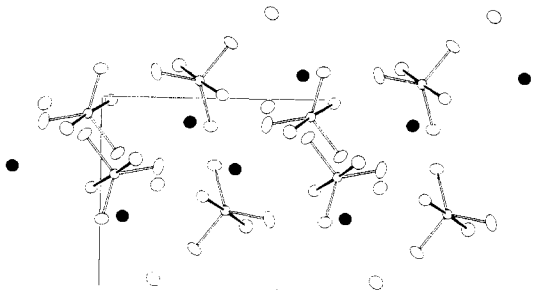

Figure 1. Projection of the structure along the *b* axis. The *a* axis is drawn horizontally and the *c* axis vertically. The black nonbonded ellipses denote K1; the white nonbonded ellipses denote K2.

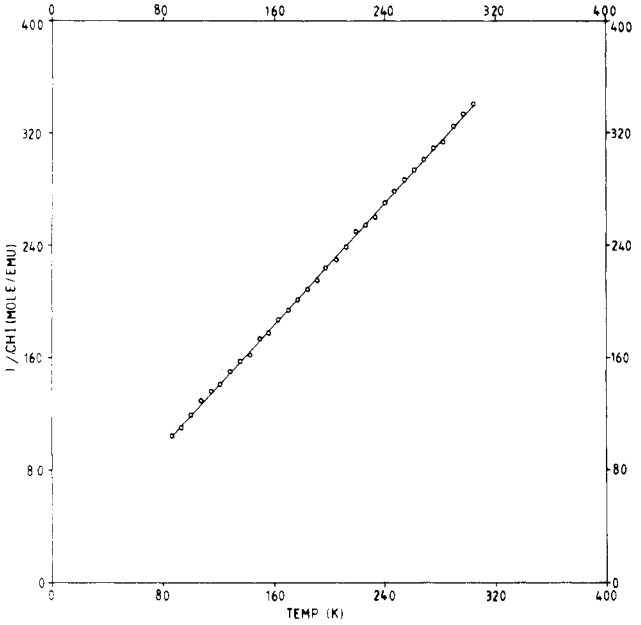

Figure 2. Plot of the $1/\chi(T)$ versus T curve of $K_2RuO_3(OH)_2$.

Both potassium ions are found in a very irregular eight-coordination with four oxygen atoms at a distance of about 2.7 Å and four at a distance of 3.0 Å.

The coordinates and the equivalent isotropic parameters of the non-hydrogen atoms are listed in Table II and the anisotropic parameters in the supplementary material. Some relevant interatomic distances and angles can be found in Table III. Figure 1 contains a plot of the crystal structure projected on the *ac* plane. Plots showing the $RuO_3(OH)_2^{2-}$ ion separately and a projection of the structure on the *ab* plane are provided in the supplementary material.

A Curie–Weiss fit to the magnetic susceptibility data (Figure 2), with a diamagnetic correction of -100×10^{-6} emu/mol, produces the following constants: $\mu_{eff} = 2.721$ (3) μ_B, $\Theta = -9.6$ K, $g = 1.923$. The g factor is calculated by assuming $S = 1$ (vide infra).

Calculations

For the MO calculation a symmetrical trigonal-bipyramidal coordination polyhedron around the ruthenium is used. Its symmetry is D_{3h}, with two Ru–O distances of 2.034 Å and three distances of 1.755 Å, in close approximation to the crystal structure determination. This was done in order to greatly simplify the calculation.

The hydrogen atoms were placed along the apical axis, at a distance of 0.95 Å from the oxygen atoms lying on this axis. For the semiempirical MO calculation the modified Wolfsberg–Helmholz method has been used. The basis set consists of the ruthenium 4d, 5s, and 5p orbitals, the oxygen 2s and 2p orbitals, and the hydrogen 1s orbital. With use of the coordinate system and numbering as in Figure 3, the symmetry-adapted orbitals as listed in Table IV can be found. The radial parts of the wave functions of ruthenium,[14] oxygen,[15] and hydrogen[16] have been obtained from the literature (Table V).

The matrix elements H_{ii} were set equal to the –VOIP's (valence orbital ionization potentials) for the different orbitals. The VOIP's are assumed to be a function of the ion charge q according to the relation

$$\mathrm{VOIP}(q) = Aq^2 + Bq + C$$

The oxygen and hydrogen parameters are listed in the literature.[17] For

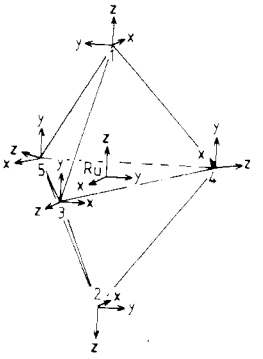

Figure 3. Coordinate system and numbering used in the MO calculation.

Table IV. Symmetry-Adapted Linear Combinations of Atomic Orbitals (D_{3h})

Oxygen σ-Orbitals

A_1': $1/2^{1/2}(s_1 + s_2)$, $1/3^{1/2}(s_3 + s_4 + s_5)$, $1/2^{1/2}(p_{z_1} + p_{z_2})$, $1/3^{1/2}(p_{z_3} + p_{z_4} + p_{z_5})$

A_2'': $1/2^{1/2}(s_1 - s_2)$, $1/2^{1/2}(p_{z_1} - p_{z_2})$

E': $[1/2^{1/2}(s_3 - s_4)$, $1/6^{1/2}(-s_3 - s_4 + 2s_5)]$
$[1/2^{1/2}(p_{z_3} - p_{z_4})$, $1/6^{1/2}(-p_{z_3} - p_{z_4} + 2p_{z_5})]$

Oxygen π-Orbitals

A_2'': $1/3^{1/2}(p_{y_3} + p_{y_4} + p_{y_5})$

E'': $[1/2^{1/2}(p_{y_3} - p_{y_4})$, $1/6^{1/2}(p_{y_3} + p_{y_4} - 2p_{y_5})]$
$[8^{1/2}/7(3^{1/2}p_{x_1} - 1/4p_{y_1} - 3^{1/2}p_{x_2} - 1/4p_{y_2})$, $8^{1/2}/7(1/4p_{x_1} + 3^{1/2}p_{y_1} - 1/4p_{x_2} + 3^{1/2}p_{y_2})]$

A_2': $1/3^{1/2}(p_{x_3} + p_{x_4} + p_{x_5})$

E': $[1/2^{1/2}(p_{x_3} - p_{x_4})$, $1/6^{1/2}(p_{x_3} + p_{x_4} - 2p_{x_5})]$
$[8^{1/2}/7(3^{1/2}p_{x_1} - 1/4p_{y_1} + 3^{1/2}p_{x_2} + 1/4p_{y_2})$, $8^{1/2}/7(1/4p_{x_1} + 3^{1/2}p_{y_1} + 1/4p_{x_2} - 3^{1/2}p_{y_2})]$

Ruthenium Orbitals

A_1': $4d_{z^2}$ E': $[4d_{x^2-y^2}, 4d_{xy}]$ E'': $[4d_{xz}, 4d_{yz}]$
A_1': 5s E': $[5p_x, 5p_y]$ A_2'': $5p_z$

Hydrogen Orbitals

A_1': $(s_1 + s_2)$ A_2'': $(s_1 - s_2)$

Table V. Radial Parts of the Wave Functions[a]

	exponent		exponent
1s	1.3	5s	2.078
2s	2.2	5p	2.043
2p	1.975		

	coeff 1	exponent 1	coeff 2	exponent 2
4d	0.5573	5.378	0.6642	2.303

[a] s and p orbitals are in a single-μ representation and d orbitals in a double-μ representation.[14-16]

Table VI. VOIP's for Ruthenium (in eV)

	Ru^0	Ru^+		Ru^0
$d^n \rightarrow d^{n-1}$	9.001		$d^np \rightarrow d^n$	4.042
$d^{n-1}s \rightarrow d^{n-2}s$	10.784		$d^{n-1}sp \rightarrow d^{n-1}s$	5.379
$d^{n-1}p \rightarrow d^{n-2}p$	10.717		$d^{n-1}p^2 \rightarrow d^{n-1}p$	
$d^ns \rightarrow d^n$	7.3689	15.632		
$d^{n-1}s^2 \rightarrow d^{n-1}s$	8.905	17.419		
$d^{n-1}sp \rightarrow d^{n-1}p$	10.004	18.263		

(14) Basch, H.; Gray, H. B. *Theor. Chim. Acta* **1966**, *4*, 367.

(15) Burns, G. *J. Chem. Phys.* **1964**, *41*, 1521.

(16) Howell, J.; Rossi, A.; Wallace, D.; Haraki, K.; Hoffman, R. Forticon 8, QCPE Program No. 344, Department of Chemistry, Cornell University: Ithaca, NY.

Table VII. VOIP Curve Parameters *A*, *B*, and *C* and Madelung Parameters

	orbital	*A*	*B*	*C*	Madelung param
H	1s	13.168	27.18	13.60	12.8
O	2s	0.0	15.20	33.0	15.2
	2p	0.0	15.20	16.4	15.2
Ru	4d[b]	1.71[a]	8.5[c]	9.001	10.7[a]
		1.71[a]	8.5[c]	10.78	
		1.71[a]	8.5[c]	10.71	
	5s[b]	0.911[a]	8.26	7.37	6.3[a]
		0.911[a]	8.57	8.91	
		0.911[a]	8.26	10.00	
	5p[b]	0.91[a]	6.96	4.04	4.5[a]
		0.91[a]	7.00[c]	5.38	
		0.91[a]	7.00[c]	5.40[c]	

[a] Values for iron obtained from ref 16. [b] Same order of configurations as in Table VI. [c] Estimated from found values, assuming the VOIP curves are parallel.[3]

ruthenium the VOIP's have been determined from atomic spectra[18] according to Viste and Gray.[3] As can be seen in Table VI, only a few VOIP's for Ru^0 and Ru^+ could be determined; it was therefore impossible to obtain all necessary *A*, *B*, and *C* parameters. However, as in general the *A* parameter is relatively small[19] and as the ruthenium charge appeared to be approximately 1.3, the error made is probably not very large. Missing parameters were estimated from listed values for iron[19] as shown in Table VII. To the H_{ii}'s also a Madelung correction was applied, with the Coulomb integrals obtained for iron.[16]

The off-diagonal elements H_{ij} were approximated by

$$H_{ij} = -F \cdot G_{ij} \cdot (H_{ii} + H_{jj})/2$$

where G_{ij} is the group overlap integral. Basch et al. showed that, for the tetrahedral anions MnO_4^{2-} (charge 2−) and MnO_4^{3-} (d^2 manganese), *F* factors of 1.78 and 1.81, respectively, gave results in good agreement with observed spectra.[19] We therefore applied an *F* factor of 1.80.

The actual corrections for overlap, the calculation and solution of the secular determinant, and the charge iteration were performed with a FORTRAN program called FORTICON8.[16] The results of the calculation are shown in Table VIII.

Discussion and Conclusions

In the compound $K_2RuO_3(OH)_2$ we have found the ruthenium atom to be coordinated by five oxygen atoms, two at a distance of 2.03 Å and three at a distance of 1.76 Å. These bond lengths are in agreement with those found in the literature, e.g. $KRuO_4$ (1.79 Å),[20] RuO_4 (1.705 Å),[21] and $BaRuO_3(OH)_2$ (1.75 and 2.03 Å).[9]

The question arises whether the structures of the two compounds $BaRuO_3(OH)_2$ and $K_2RuO_3(OH)_2$ are related. The averaged structure of $BaRuO_3(OH)_2$, described by Nowogrocki, can be transformed from hexagonal ($P6_3/mmc$, $a = 5.787$ Å, $c = 25.471$ Å) to an orthorhombic setting as follows: $a' = {}^1/_3c$, $b' = 2b + a$, $c' = -a$ plus an origin shift over $(-{}^1/_4, {}^1/_2, {}^1/_4)$. This results in a unit cell with the axes $a = 8.491$ Å, $b = 10.023$ Å, and $c = 5.707$ Å, which is close to the dimensions of the $K_2RuO_3(OH)_2$ unit cell. It can be shown that the $RuO_3(OH)_2^{2-}$ entities are shifted over approximately 0.8 Å and rotated with respect to each other whereas the Ba and K positions are almost the same (the other K occupying the remaining voids). It can thus be concluded that the two structures can be transformed into each other by substitution of 1 Ba^{2+} + 1 vacancy by 1 K^+ + 1 K^+ and reorientation of the $RuO_3(OH)_2^{2-}$ group.

In $K_2RuO_3(OH)_2$, the shortest O–O distance between two apical oxygens of different ruthenate ions is 2.82 Å. As in $K_2OsO_2(OH)_4$, with an O–O distance[22] of 2.79 Å, this must surely give rise to hydrogen bridging, in contrast to the case for $BaRuO_3(OH)_2$, where the O–O distance is 3.02 Å.

Table VIII

(a) Results from MO Calculations

Corrected VOIP's (in eV, Madelung Correction Included)

1s	7.43	4d	2.96
2s	19.90 (eq),[a] 20.54 (ap)	5s	1.14
2p	3.30 (eq), 3.94 (ap)	5p	−2.21

Charges

Ru	1.31	ap O	−0.68
eq O	−0.76	H	0.17

Ground-State Orbital Configurations

Ru	$4d^{5.26}5s^{0.45}5p^{0.98}$	ap O	$2s^{1.63}2p^{5.05}$
eq O	$2s^{1.81}2p^{4.95}$	H	$1s^{0.83}$

(b) Ground-State Energy Levels (in eV)

sym	energy	occupancy	sym	energy	occupancy
$7a_1'$	34.75	0	4e′	−3.50	4
6e′	32.91	0	3e′	−4.26	4
$6a_1'$	25.01	0	$4a_1'$	−4.76	2
$5a_2''$	24.84	0	2e′	−5.36	4
$4a_2''$	22.43	0	1e″	−5.59	4
$5a_1'$	4.02	0	$2a_2''$	−7.90	2
5e′	1.31	0	$3a_1'$	−8.53	2
3e″	−0.34	2	1e′	−20.44	4
$1a_2'$	−3.16	2	$2a_1'$	−20.89	2
$3a_2''$	−3.18	2	$1a_2''$	−22.67	2
2e″	−3.28	4	$1a_1'$	−22.96	2

[a] eq denotes equatorial; ap denotes apical.

From the MO calculations it follows that the ordering of the valence orbitals is 3e″, 5e′, $5a_1'$, very different from the previously found ordering e, t_2, originating from the assumption of tetrahedral coordination.

Both a crystal field calculation and the MO calculation show that the ground-state configuration is $(3e'')^2$, leading to the terms $^3A_2' + {}^1E' + {}^1A_1'$. As in a first-order approximation the ground-state term $^3A_2'$ is not subject to spin–orbit coupling, we should expect from the magnetic susceptibility data a *g* value of 2.00. In a second-order approximation, however, there is spin–orbit coupling with wave functions originating from the excited levels 5e′ and $5a_1'$ and therefore the *g* value is somewhat smaller, $g = 1.93$. Moreover, since excited states originating from electron–electron repulsion within the ground-state configuration usually are not much populated at room temperature, the diamagnetic states $^1E'$ and $^1A_1'$ do not lower the *g* value in the temperature range where the magnetic susceptibility data are collected. Therefore, the conclusion is made that the decrease in the *g* factor is mainly caused by second-order spin–orbit coupling. The occurrence of a nonzero Θ value most likely originates from zero-field splitting of the ground-state term (which is always the case in an $S = 1$ system), and possibly also from a small antiferromagnetic coupling between the ruthenate ions.

The MO calculation shows that the more complete ground-state configuration is $(3a_2'')^2(1a_2')^2(3e'')^2$ with the lowest lying term being $^3A_2'$. In a tetrahedral complex this is $(t_1)^6(e_1)^2$, also with the lowest lying term $^3A_2$. It has been shown[5] that the formerly assumed tetrahedral ruthenate ion should exhibit two transitions: $^3A_2 \rightarrow {}^3T_1$ (e → t_2) and $^3A_2 \rightarrow {}^3T_1$ (t_1 → e) with calculated transition energies 1.49 and 3.08 eV, respectively. However, the ruthenate ion shows only one peak in its visible–UV spectrum[10] at 21 600 cm^{-1} (2.67 eV).

The corresponding excited states in our model are $(3e'')^1(5e')^1$ and $(3a_2'')^1(3e'')^3$ at 1.65 and 2.84 eV, respectively. Electric dipole transitions are allowed between the terms $^3A_2' \rightarrow {}^3A_1''$ (3e″ → 5e′) and $^3A_2' \rightarrow {}^3E'$ ($3a_2' \rightarrow 3e''$). The charge-transfer transition

(17) McGlynn, S. P.; Vanquickenborne, L. G.; Konoshita, M.; Carroll, P. G. *Introduction to Applied Quantum Chemistry*; Holt, Rinehart and Winston: New York, 1972; pp 423–431.
(18) Moore, C. E. *Atomic Energy Levels*; NBS Circular 467; National Bureau of Standards: Washington, DC, 1952; Vol. III.
(19) Basch, H.; Viste, A.; Gray, H. B. *J. Chem. Phys.* **1966**, *44*, 10.
(20) Silverman, M. D.; Levy, H. A. *J. Am. Chem. Soc.* **1954**, *76*, 3317.
(21) Schäfer, L.; Seip, H. M. *Acta Chem. Scand.* **1967**, *21*, 737.
(22) Atovmyan, L. O.; Andrianov, V. G.; Porai-Koshits, M. A. *Zh. Strukt. Khim.* **1962**, *3*, 685.

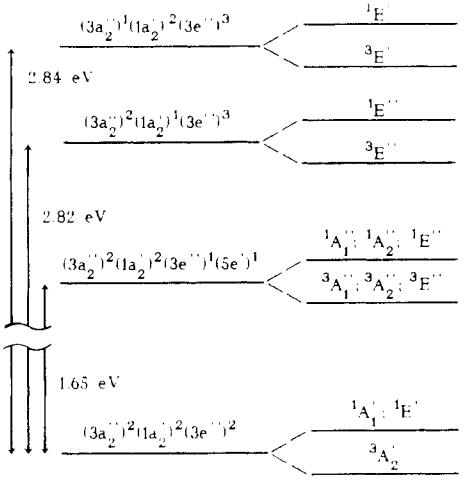

Figure 4. Plot of the ground state and some relevant excited states according to the MO calculation. The terms with the same spin multiplicity, which originate from one configuration, have been drawn schematically at the same level.

$^3A_2' \rightarrow {}^3E''$ ($1a_2' \rightarrow 3e''$) is electric dipole forbidden (Figure 4). If no corrections are made for electron–electron repulsion, then the calculated transition energies are given as above.

Although at 1.65 eV no band has been observed, the transition energy value of 2.84 eV is in rather good agreement with the observed value of 2.67 eV, in contrast to the value of 3.08 eV that has been found earlier with the more advanced HFS–DVM method,[5] starting from a tetrahedral environment. However, the possibility that the calculated 1.65-eV transition should be assigned to the observed band may not be excluded, as the accuracy of the Wolfsberg–Helmholz method is not very well established. Nevertheless, we assume that the lack of resemblance between calculated and observed spectra of ruthenate in the past was mainly due to the assumption of tetrahedral coordination for the ruthenium ion.

It may be very interesting to verify if the found coordination occurs in other ruthenates. Nowogrocki[9] et al. found certain similarities between $SrRuO_4 \cdot H_2O$ and $BaRuO_3(OH)_2$, and also the compound $NaRuO_4 \cdot H_2O$ would be a very interesting compound[3] to study.

For one perruthenate, $KRuO_4$, the structure was determined to be of the scheelite ($CaWO_4$) type.[20] However, this compound does not contain a H_2O unit, and therefore $NaRuO_4 \cdot H_2O$ should not necessarily show the scheelite structure and thus is a probable candidate to exhibit the five-coordination. If this trigonal-bipyramidal configuration is found, the compound, containing a d^1 ion, might be subject to a Jahn–Teller distortion.

Acknowledgment. We wish to express our gratitude to Dr. R. A. G. De Graaff for his helpful suggestions during the crystal structure determination and to the first reviewer for his remark, leading to the selection of the correct enantiomorph. The investigations were supported in part (W.G.H.) by the Netherlands Foundation for Chemical Research (SON) with financial aid from the Netherlands Organization for the Advancement of Pure Research (ZWO).

Registry No. $K_2RuO_3(OH)_2$, 112113-56-1.

Supplementary Material Available: Table SI, listing the anisotropic thermal parameters, and Figures SI and SII, showing the coordination of the ruthenium and a projection of the structure on the *ab* plane, respectively (3 pages); Table SII, listing the observed and calculated structure factors (12 pages). Ordering information is given on any current masthead page.

Contribution from the Department of Chemistry and Chemical Physics Program, Washington State University, Pullman, Washington 99163, and Gorlaeus Laboratories, Leiden University, P.O. Box 9502, 2300 RA Leiden, The Netherlands

Crystal Structures of Three Phases of Tetramethylammonium Trichlorocuprate(II) (TMCuC)

Roger D. Willett,*† Marcus R. Bond,† W. G. Haije,‡ O. P. M. Soonieus,‡ and W. J. A. Maaskant‡

Received May 1, 1987

The compound tetramethylammonium trichlorocuprate(II), $C_4H_{12}NCuCl_3$, exhibits two crystalline phase transitions, one at 319 K and the other at 373 K. X-ray structure determinations of the three corresponding phases were carried out at 213.2 (3), 323 (2), and 405 (2) K. These structures are deformed members of the hexagonal perovskite family (2L): crystal data at 213 K, monoclinic $P2_1$, a = 8.948 (8) Å, b = 32.225 (10) Å, c = 8.980 (2) Å, β = 119.487 (18)°; crystal data at 323 K, triclinic $P\bar{1}$, a = 9.082 (5) Å, b = 9.073 (5) Å, c = 6.442 (3) Å, α = 90.05 (4)°, β = 92.40 (4)°, γ = 119.99 (3)°; crystal data at 405 K, hexagonal $P6_3/mmc$, $a = b$ = 9.160 (2) Å, c = 6.474 (2) Å. In the high-temperature phase (2L) the Jahn–Teller elongation is disordered over three possible configurations, x, y, and z, in the intermediate-temperature phase (2L) one site is ordered (z) and the other is disordered over two configurations (x and y), and the low-temperature phase (10L) exhibits a static structure as far as the Jahn–Teller effect is concerned. All phases show disorder of the tetramethylammonium group except for the low-temperature phase, which is partially ordered with respect to this ion. This means that there must be another phase at lower temperature.

Introduction

One class of structural types exhibited by $ACuCl_3$ salts (A = monopositive cation)[1] is a Jahn–Teller-distorted version of the $CsNiCl_3$ structure.[2] The latter contains parallel chains of face-sharing $NiCl_6$ octahedra separated by the Cs cations (see Figure 1). In the copper(II) salts, the octahedra assume a tetragonally elongated 4 + 2 coordination geometry such that each Cu^{2+} ion has four short (~2.3-Å) and two long (2.8–3.2-Å) Cu–Cl bonds. The neighboring Cu^{2+} ions are linked by one symmetrical Cu–Cl–Cu bridge (both Cu–Cl bonds ~2.3 Å) and two asymmetrical bridges involving one short and one long Cu–Cl bond. Cu–Cl–Cu bridges involving two long Cu–Cl bonds are energetically unfavorable and have not been observed experimentally. This introduces a cooperative nature into the Jahn–Teller distortions within the chain structure whereas the cooperative nature between the chains originates from the elastic interactions via the close-packed Cl layers. Any individual $CuCl_6$ octahedron can undergo a Jahn–Teller elongation along one of its three "4-fold" axes; however, the distortion assumed by this octahedron is now

† Washington State University.
‡ Leiden University.

(1) Willett, R. D.; Geiser, U. *Croat. Chem. Acta* **1984**, *57*, 737.
(2) Tishchenko, G. N. *Tr. Inst. Kristallogr., Akad. Nauk SSSR* **1955**, *11*, 93; *Gmelins Handbuch der Anorganischen Chemie*, 8th ed.; Springer-Verlag: New York, 1966; Nickel Compounds B-3, p 1103.

